JOURNAL OF THE AMERICAN COLLEGE OF CARDIOLOGY
VOL. 64, NO. 8, 2014

ISSN 0735-1097/$36.00
PUBLISHED BY ELSEVIER INC.
http://dx.doi.org/10.1016/j.jacc.2014.06.1155

The Symptom Complex of Familial Sinus Node Dysfunction and Myocardial Noncompaction Is Associated With Mutations in the HCN4 Channel

Patrick A. Schweizer, MD,*† Julian Schröter, BSc,*‡ Sebastian Greiner, MD,* Jan Haas, PhD,*† Pessah Yampolsky, PhD,* Derliz Mereles, MD,* Sebastian J. Buss, MD,* Claudia Seyler, PhD,* Claus Bruehl, PhD,‡ Andreas Draguhn, MD,‡ Michael Koenen, PhD,*‡§ Benjamin Meder, MD,*† Hugo A. Katus, MD,*† Dierk Thomas, MD*†

ABSTRACT

BACKGROUND Inherited arrhythmias were originally considered isolated electrical defects. There is growing evidence that ion channel dysfunction also contributes to myocardial disorders, but genetic overlap has not been reported for sinus node dysfunction (SND) and noncompaction cardiomyopathy (NCCM).

OBJECTIVES The study sought to investigate a familial electromechanical disorder characterized by SND and NCCM, and to identify the underlying genetic basis.

METHODS The index family and a cohort of unrelated probands with sinus bradycardia were examined by electrocardiography, Holter recording, exercise stress test, echocardiography, and/or cardiac magnetic resonance imaging. Targeted next-generation and direct sequencing were used for candidate gene analysis and mutation scanning. Ion channels were expressed in HEK293 cells and studied using patch-clamp recordings.

RESULTS SND and biventricular NCCM were diagnosed in multiple members of a German family. Segregation analysis suggested autosomal-dominant inheritance of the combined phenotype. When looking for potentially disease-causing gene variants with cosegregation, a novel hyperpolarization-activated cyclic nucleotide channel 4 (*HCN4*)-G482R mutation and a common cysteine and glycine-rich protein 3 (*CSRP3*)-W4R variant were identified. *HCN4*-G482R is located in the highly conserved channel pore domain. Mutant subunits were nonfunctional and exerted dominant-negative effects on wild-type current. *CSRP3*-W4R has previously been linked to dilated and hypertrophic cardiomyopathy, but was also found in healthy subjects. Moreover, different truncation (695X) and missense (P883R) *HCN4* mutations segregated with a similar combined phenotype in an additional, unrelated family and a single unrelated proband respectively, which both lacked *CSRP3*-W4R.

CONCLUSIONS The symptom complex of SND and NCCM is associated with heritable HCN4 defects. The NCCM phenotype may be aggravated by a common CSRP3 variant in one of the families. (J Am Coll Cardiol 2014;64:757–67)

From the *Department of Cardiology, University of Heidelberg, Heidelberg, Germany; †DZHK (German Centre for Cardiovascular Research), partner site Heidelberg/Mannheim, University of Heidelberg, Heidelberg, Germany; ‡Institute for Physiology and Pathophysiology, University of Heidelberg, Heidelberg, Germany; and the §Department of Molecular Neurobiology, Max-Planck-Institute for Medical Research, Heidelberg, Germany. This work was supported in part by grants from the Max-Planck-Society (TANDEM project to Drs. Schweizer and Koenen), the German Cardiac Society (research scholarship to Dr. Yampolsky), the Medical Faculty of the University of Heidelberg (Young Investigator Award to Dr. Yampolsky), the German Cardiac Society and the Hengstberger Foundation (Klaus-Georg and Sigrid Hengstberger Scholarship to Dr. Thomas), and the Joachim Siebeneicher Foundation (to Dr. Thomas). All authors have reported that they have no relationships relevant to the content of this paper to disclose.
Listen to this manuscript's audio summary by *JACC* Editor-in-Chief Dr. Valentin Fuster.
You can also listen to this issue's audio summary by *JACC* Editor-in-Chief Dr. Valentin Fuster.

Manuscript received February 26, 2014; revised manuscript received May 26, 2014, accepted June 2, 2014.

ABBREVIATIONS AND ACRONYMS

CMR = cardiac magnetic resonance imaging

CS = cover slips

CSRP3 = cysteine and glycine-rich protein 3

HCN = hyperpolarization-activated cyclic nucleotide channel

LVEF = left ventricular ejection fraction

MVP = mitral valve prolapse

NCCM = noncompaction cardiomyopathy

NGS = next-generation sequencing

SAN = sinoatrial node

SND = sinus node dysfunction

Noncompaction cardiomyopathy (NCCM) is characterized by excessive ventricular hypertrabeculation and complicated by heart failure, arrhythmia, and thromboembolic events (1). Mutations in genes encoding sarcomeric, cytoskeletal, Z-disk, chaperone, Notch-pathway, or nuclear membrane proteins have been related to the disorder (2–5). However, a comprehensive analysis of the genetic basis of NCCM is not available to date, and genotype-phenotype correlations are poorly understood (2).

SEE PAGE 768

Sinus node dysfunction (SND) is associated with syncope or bradyarrhythmic death and frequently requires cardiac pacemaker implantation. The hyperpolarization-activated cyclic nucleotide channel 4 (HCN4) is a major constituent of the pacemaker current (I_f) in the sinoatrial node (SAN) and contributes significantly to spontaneous diastolic depolarization (6–8). Accordingly, mutations in the *HCN4* gene were associated with familial forms of SND (9–12). Abnormalities of SAN function are particularly common in heart failure, suggesting a genetic and mechanistic link between electrical and structural dysfunction (13). Indeed, the depolarizing cardiac sodium channel gene *SCN5A* and non-ion channel genes *MYH6* and *CASQ2* have recently been implicated in the pathogenesis of both SND and structural heart disease (14–16). However, genetic overlap between SND and NCCM has not been previously described.

In this paper, we report on a symptom complex comprising SND and NCCM observed in 2 unrelated families and in an additional unrelated proband. In a candidate gene approach, we identified a novel *HCN4*-G482R loss-of-function mutation that segregated with all affected members in the index family. In addition, a common cysteine and glycine-rich protein 3 (*CSRP3*)-W4R variant that has previously been found in dilated and hypertrophic cardiomyopathy patients and in healthy subjects (17–19) cosegregated with the clinical syndrome in the family. Furthermore, multiple members of a previously reported family (11) and an unrelated proband exhibited similar combined phenotypes and carried truncation (695X) (11) and missense (P883R) *HCN4* mutations, respectively, but lacked *CSRP3*-W4R.

Our results confirm a primary role of HCN4 channels in cardiac pacemaker function and in SND. Furthermore, the data give rise to the notion that HCN4 channels are implicated in the formation of ventricular structure and may contribute to the development of NCCM when dysfunctional.

METHODS

A detailed description of the methods is provided in the Online Appendix.

PATIENTS AND CLINICAL INVESTIGATIONS. Patients were evaluated by clinical examination, 12-lead electrocardiogram (ECG), 24-h Holter recording, exercise test, echocardiography, and cardiac magnetic resonance imaging (CMR). Holter recordings were pre-analyzed using H-Scribe 4.0 software (Mortara, Essen, Germany) and validated by an electrophysiologist. All patients provided written informed consent prior to clinical and genetic investigations. The Ethics Committee of Heidelberg University (Germany) approved the research protocol, and the investigation conforms to the principles outlined in the Declaration of Helsinki.

CANDIDATE GENE ANALYSIS AND VALIDATION IN THE INDEX FAMILY. Targeted next-generation sequencing (NGS) and direct sequencing were employed in the index family to analyze genes commonly involved in cardiomyopathies and heart rhythm disorders (Online Table 1). NGS was performed on an Illumina HiSeq2000 (Illumina, San Diego, California) using the paired end 2x100bp method (Online Appendix). Variations present in the publicly available variant database "dbSNP137common" and flagged as validated by frequency, indicating an allele frequency of ≥1% in populations, were considered to have a benign effect and therefore were excluded from further analysis. Other genetic variants were retained and tested for segregation in the family by Sanger sequencing.

COMPREHENSIVE MUTATION SCANS IN A SINUS BRADYCARDIA COHORT. We carried out comprehensive mutation scans of *HCN4* using direct exon sequencing in a cohort of 86 unrelated patients diagnosed with sinus bradycardia. Study subjects were included in the cohort when resting heart rates and minimum heart rates were <60 and <40 beats/min, respectively. Probands with prolonged QT intervals or ischemic heart disease were excluded. Sequencing of the exon harboring the *HCN4* mutation was then performed in relatives of each proband to determine their mutation carrier status. Probands and their families diagnosed with a combined phenotype of sinus bradycardia and myocardial noncompaction also were tested for carrying *CSRP3*-W4R by direct sequencing.

MUTAGENESIS. Site-directed mutagenesis (QuikChange II Site-Directed Mutagenesis Kit, Stratagene, La Jolla,

California) was performed to introduce the G482R mutation into the human *HCN4* gene (GenBank accession number NM_005477). Automated DNA sequence analysis (GATC Biotech, Konstanz, Germany) verified the mutation.

CELL CULTURE. Human embryonic kidney cells (HEK293) were grown on glass cover slips (CS) (3×10^4 cells per CS) in Dulbecco's Modified Eagles's Medium supplemented with 2 mM glutamine, 10% fetal calf serum, 100 U/ml penicillin-G sodium, and 100 mg/ml streptomycin sulfate in 5% CO_2 at 37°C. Cells were transfected using the calcium-phosphate method with 0.6 μg plasmid DNA per CS encoding mutant or wild-type HCN4 channel subunits. Successful transfection was visualized by coexpressed CD8 antigen (0.1 μg DNA/CS) identified by anti-CD8 antibody-coated dynabeads (Life Technologies, Carlsbad, California). In coexpression experiments, equal amounts (0.3 μg) of mutant and wild-type DNA were used (11).

CELLULAR ELECTROPHYSIOLOGY. Membrane currents were recorded 1 to 2 days after transfection under voltage-clamp conditions (whole-cell configuration) at room temperature (21°C to 23°C) as published (11). Functional properties of HCN4 channels were investigated employing different voltage protocols as reported (11,20).

STATISTICS AND DATA ANALYSIS. Electrophysiological data were recorded and analyzed offline using Signal software (Version 4.05; CED, Cambridge, England). GraphPad Instat (Version 3.06; La Jolla, California) was used for statistical analyses. All results are provided as mean ± SEM. Data were tested for normality (Kolmogorov-Smirnov test), and a 2-tailed unpaired Student *t* test, followed by a Welch correction to account for unequal variances was used for statistical comparisons. A Mann-Whitney test was performed for comparison of current densities (molecular electrophysiology) that did not follow Gaussian distributions. A p value <0.05 was considered statistically significant.

RESULTS

CLINICAL CHARACTERISTICS OF INDEX FAMILY. The 23-year-old index patient of family A (IV.1) (Fig. 1A) presented with syncope resulting in a car accident. He complained dizziness, fatigue, palpitations, and was aware of bradycardia since childhood. Resting 12-lead electrocardiogram showed sinus bradycardia, first-degree atrioventricular block, and T-wave inversions in the inferior leads (Fig. 2A). The QTc interval was normal (Table 1). Holter recording

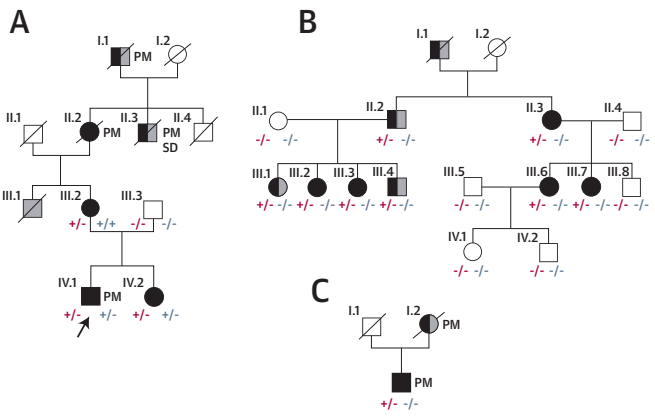

FIGURE 1 Pedigrees of Families Affected by SND and NCCM Associated With *HCN4* Mutations

(A) Index family A carrying the novel *HCN4*-G482R mutation. **(B)** Family B with members heterozygously affected by the *HCN4*-695X mutation (11). **(C)** Pedigree of the single proband heterozygous for *HCN4*-P883R. **Closed** symbols indicate affected family members, **open** symbols denote unaffected family members, and **gray** symbols indicate unknown phenotype. **Left half** of symbol indicates status concerning sinus bradycardia, and **right half** of symbol reflects myocardial noncompaction status. The index patient is denoted by an **arrow**. **Circles** refer to women, and **squares** indicate men. Individuals that received an electronic cardiac pacemaker are marked by PM, and SD indicates individuals that experienced sudden death. **Slashed** symbols indicate deceased subjects with an unknown genotype and phenotypic characterization based on medical records and family history. **Red** signs indicate respective *HCN4* mutation status, and **slate** signs reflect *CSRP3*-W4R genotype (plus symbol indicates carrier of mutant allele, minus symbol denotes wild-type allele). HCN = hyperpolarization-activated cyclic nucleotide channel; CSRP = cysteine and glycine-rich protein; NCCM = noncompaction cardiomyopathy; SND = sinus node dysfunction.

demonstrated minimum and average heart rates of 21 and 34 beats/min, respectively (Figs. 2B and 2C, Table 1). Exercise testing revealed impaired chronotropic capacity, intermittent ectopic atrial rhythms, and ventricular bigeminy (Figs. 2D and 2E). In addition to the electrical phenotype, transthoracic echocardiography exhibited biventricular hypertrabeculation that met diagnostic criteria of left ventricular noncompaction, according to Jenni or Chin (21), and mitral valve prolapse (MVP) (Figs. 3A and 3D, Online Video 1). Pronounced intracavitary trabeculations and perfused intertrabecular recesses were apparent in right and left ventricular walls (Figs. 3A and 3D, Online Videos 1 and 2), and basal left ventricular longitudinal strain was attenuated (Online Table 2). CMR confirmed that noncompacted segments mainly involved apical, lateral, and inferior walls of the left ventricle (Figs. 4A and 4B). Left ventricular ejection fraction (LVEF) was preserved despite significant noncompaction (Table 1). The patient received a dual chamber pacemaker. During

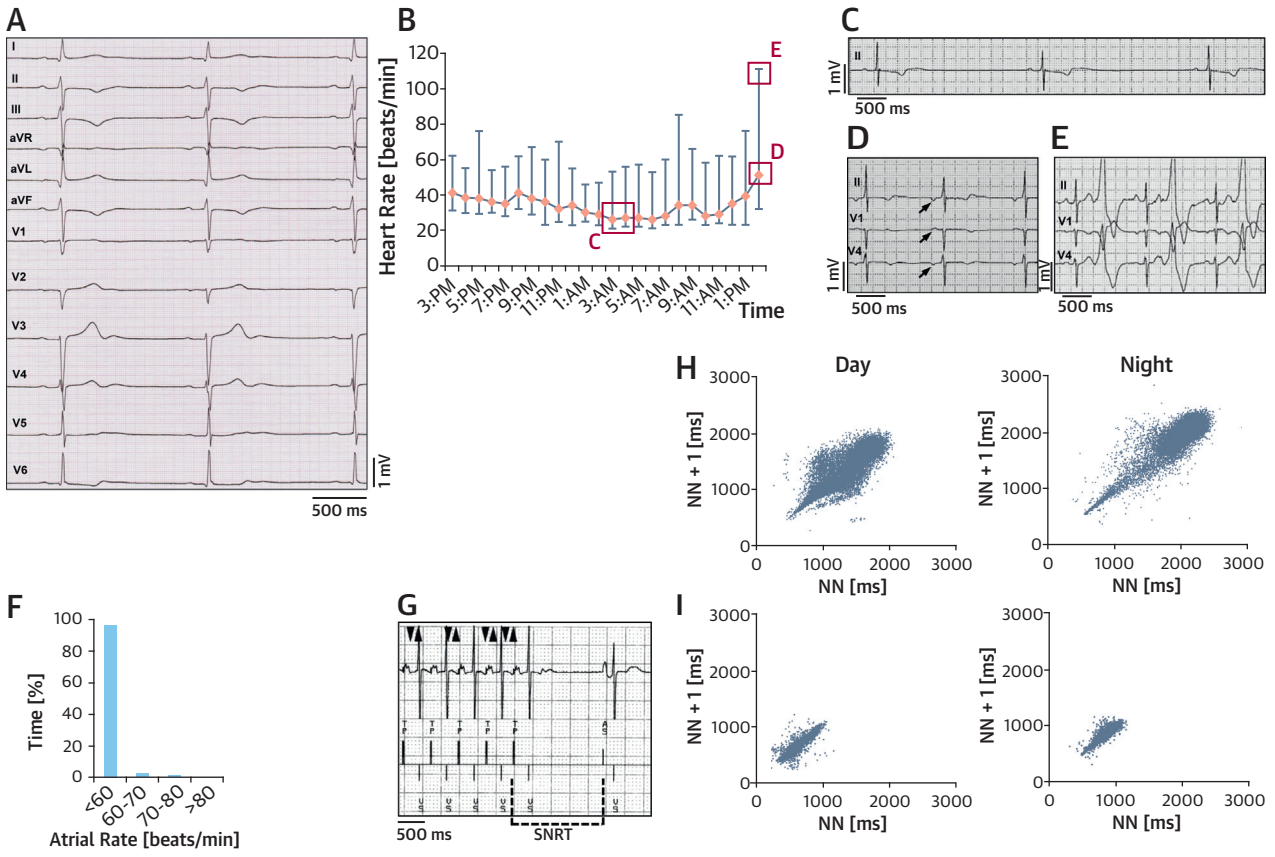

FIGURE 2 **Electrophysiological Characteristics of Index Family Members**

(A) Standard 12-lead electrocardiography of the index patient (VI.1) demonstrating sinus bradycardia. **(B)** Heart rate profile of VI.1 monitored by 24-h Holter recording shows hourly values for average, maximum, and minimum heart rate, respectively. **(C)** Minimum heart rate (21 beats/min) recorded at night. **(D, E)** During exercise, the patient exhibited ectopic atrial rhythms **(D)** and ventricular bigeminy **(E)**. The **arrow** indicates altered P-wave polarity. **(F)** Atrial rate histograms obtained during pacemaker follow-up 6 months after implantation. **(G)** Sinus node recovery time determined via the implanted pacemaker. **(H, I)** Illustration of heart rate variability during day **(left panels)** and night **(right panels)** Holter recording. **(H)** Poincaré plots of patient VI.2 display comet-shaped patterns reflecting increased beat-to-beat dispersion. At night, NN intervals markedly exceeded 2,000 ms. **(I)** Plots of a healthy individual for comparison (modified from Schweizer et al. [11]). NN = interval between successive heart beats in the Holter recording.

6-month follow-up he did not report any recurrence of symptoms. Pacemaker interrogation revealed that atrial rates were below 60 beats/min during 96.8% of the follow up period, and sinus node recovery time was prolonged (1,900 ms; corrected sinus node recovery time, 650 ms) (**Figs. 2F and 2G**).

Family analysis (**Fig. 1A**) identified the patient's sister (IV.2; 16 years of age) (**Figs. 2H and 2I**, **Figs. 3B and 3E**, Online Videos 3 and 4, **Fig. 4C**, **Table 1**, Online Table 2) and mother (III.2; 45 years of age) (**Figs. 3C and 3F**, Online Videos 5 and 6, **Table 1**, Online Table 2), as affected by the symptom complex comprising SND, NCCM, and MVP. Of note, no extracardiac anomalies were apparent, and none of the patients actively practiced or had a history of endurance sports that might explain a vagotone-mediated sinus bradycardia. Advanced functional echocardiographic analyses revealed impaired apical rotation (22) in all affected family members (Online Fig. 1). Patient III.2 showed impaired LVEF and symptomatic heart failure (New York Heart Association functional class II to III), while patient IV.2 exhibited preserved LVEF similar to the index patient (**Table 1**). No overlap with other cardiomyopathies was observed. Clinically affected patients did not receive any medication at the time of evaluation. The father (III.3) of the index patient exhibited impaired LVEF due to myocardial infarction 5 years prior and was treated according to current guidelines. Clinical evaluation showed normal sinus node function and

TABLE 1 Baseline Characteristics of Living Members of the Index Family

Patient #	Sex	Age (yrs)	Electrocardiography			Holter Recording			HRV kSD (ms)	NYHA	LVEF (%)	NC Segm.	Syncope	Device	Combined Phenotype	Genotype (*HCN4*-G482R, *CSRP3*-W4R)	Structural Disease	Other Diagnoses
			HR (beats/min)	PR (ms)	QTc (ms)	Min HR (beats/min)	Max HR (beats/min)	Average HR (beats/min)										
III.2	f	48	46	178	419	30	118	51	286	II to III	42	15/17	No	No	Affected	Carrier	NCCM, PMV	–
III.3	m	52	64	170	393	48	155	63	164	II	46	0/17	No	No	Nonaffected	Noncarrier	IHD	Myocardial infarction
VI.1	m	23	37	208	402	21	111	34	401	I	55	8/17	Yes	PM	Affected	Carrier	NCCM, PMV	–
VI.2	f	16	36	173	400	24	132	38	449	I	61	11/17	Yes	No	Affected	Carrier	NCCM, PMV	–

CSRP = cysteine and glycine-rich protein; HCN = hyperpolarization-activated cyclic nucleotide channel; HR = heart rate; HRV = heart rate variability; IHD = ischemic heart disease; kSD = Kleiger standard deviation; LVEF = left ventricular ejection fraction as evaluated by echocardiography; NC Segm. = number of noncompacted wall with NC/C ratio > 2.0 according to Jenni or Chin (21) evaluated by echocardiography; NCCM = noncompaction cardiomyopathy; NYHA = New York Heart Association functional class; PM = pacemaker; PMV = mitral valve prolapse.

no signs of myocardial noncompaction (**Table 1**, Online Table 2, **Fig. 3**, Online Video 7). Furthermore, the grandmother (II.2), granduncle (II.3), and great-grandfather (I.1) on the maternal side of the index patient had a history of sinus bradycardia and congestive heart failure, and they had received pacemakers implanted between 40 to 50 years of age. Patients I.1 and II.2 died from stroke at 73 and 54 years of age, respectively, while patient II.3 experienced sudden death at 50 years of age. As these probands had passed away at the time of family assessment, they were not available for further clinical or genetic analysis.

GENETIC ANALYSIS IN THE INDEX FAMILY. Candidate analysis of genes commonly involved in cardiomyopathies and cardiac arrhythmias (Online Table 1) was carried out in the index family using targeted next-generation and direct Sanger sequencing. We found 593 variants in the index patient (**Fig. 1A**). No truncating variant was identified. Filtering out noncoding, synonymous, and benign variants present in the dbSNP137 common database yielded 9 nonsynonymous variants that were validated and tested in the family for segregation by Sanger sequencing. Disease relevant segregation compatible with an autosomal recessive trait was not observed (e.g., no variant was homozygously shared by the affected individuals). However, pedigree analysis (**Fig. 1A**) suggested autosomal dominant inheritance. Six heterozygous variants were detected in the index patient and shared by other family members (Online Table 3). Of those, 2 variants (*HCN4*-G482R and *CSRP3*-W4R) were detected in each family member showing the combined phenotype (III.2, VI.1, and VI.2) but not in the nonaffected father (III.3) (**Fig. 1A**). The novel *HCN4* variant was heterozygously carried by all affected family members and absent from 566 unrelated controls. It results in replacement of a glycine residue with arginine and is located in the highly conserved Glycine-Tyrosine-Glycine motif of the channel pore (G482R) (**Figs. 5A to 5D**). Furthermore, patient III.2 was homozygous for the common *CSRP3*-W4R variant (19), while her son (VI.1) and daughter (VI.2) were heterozygous.

PREVALENCE OF MYOCARDIAL NONCOMPACTION IN A SINUS BRADYCARDIA COHORT. We investigated a cohort of 86 unrelated probands with sinus bradycardia by comprehensive echocardiography and/or CMR and discovered 3 individuals that exhibited myocardial noncompaction. Interestingly, we found mutations in the exon sequence of *HCN4* in all 3 probands affected by the combined phenotype within this cohort. In addition to the index patient of

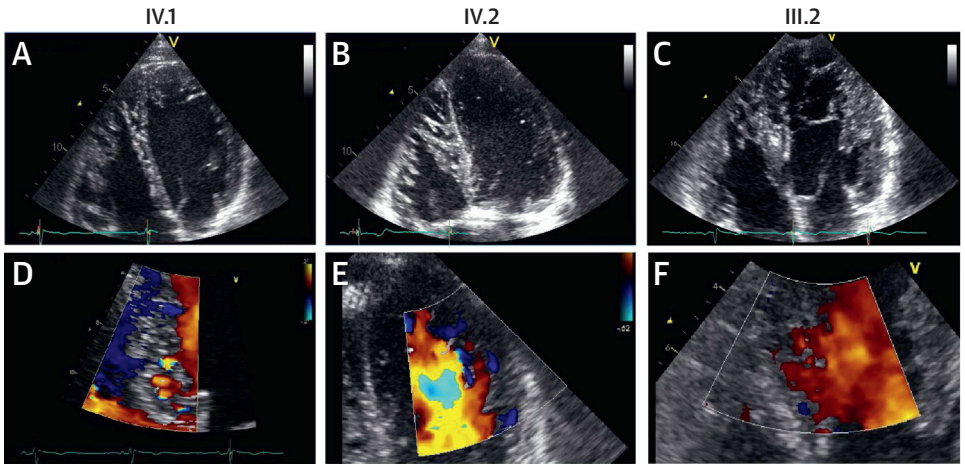

FIGURE 3 Echocardiographic Characteristics

Transthoracic apical end-diastolic views **(top)** and perfusion indicated by color-coded duplex imaging **(bottom)** of family A: patients IV.1 (**A, D,** Online Videos 1 and 2), IV.2 (**B, E,** Online Videos 3 and 4), and III.2 (**C, F,** Online Videos 5 and 6) illustrate myocardial noncompaction. For comparison please refer to the transthoracic echocardiography cine sequences of nonaffected family member III.3 (Online Video 7).

family A, who was heterozygous for *HCN4*-G482R and *CSRP4*-W4R (**Fig. 1A**), a patient and multiple members of his family carried the previously reported *HCN4*-695X mutation (11) (**Fig. 1B**, Online Fig. 2). Furthermore, in another unrelated patient, we detected a heterozygous *HCN4*-P883R mutation (**Fig. 1C**, Online Fig. 3) that was absent from 566 unrelated controls. However, the *CSRP3*-W4R variant was not present in any of these 2 latter probands and their families, respectively.

PATIENTS CARRYING *HCN4*-695X AND *HCN4*-P883R EXHIBIT COMBINED PHENOTYPES. We observed biventricular hypertrabeculation in multiple members of the previously reported family affected by the *HCN4*-695X mutation (11) (**Fig. 1B**, Online Fig. 2). Although LVEF was preserved and no overt structural abnormalities were initially noted (11), all family members carrying *HCN4*-695X that were examined by multi-modal imaging exhibited biventricular hypertrabeculation (Online Fig. 2) and MVP. The patient that heterozygously carried the *HCN4*-P883R mutation (**Fig. 1C**, Online Fig. 3) presented with sinus bradycardia (35 to 40 beats/min) and paroxysmal atrial fibrillation (bradycardia-tachycardia syndrome) and required pacemaker implantation. Echocardiography/CMR revealed myocardial noncompaction with preserved LVEF resembling the combined phenotype of the aforementioned *HCN4* mutation carriers.

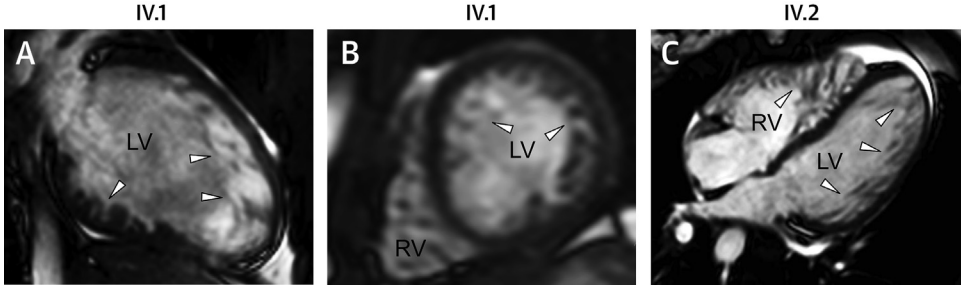

FIGURE 4 Biventricular Noncompaction Visualized by Cardiac Magnetic Resonance Imaging

Representative end-diastolic 2-chamber **(A)** and short-axis views **(B)** of the index patient (family A, VI.1). **(C)** Four-chamber view of proband IV.2, family A. **Arrows** indicate areas of prominent intracavitary trabeculations. LV = left ventricle; RV = right ventricle.

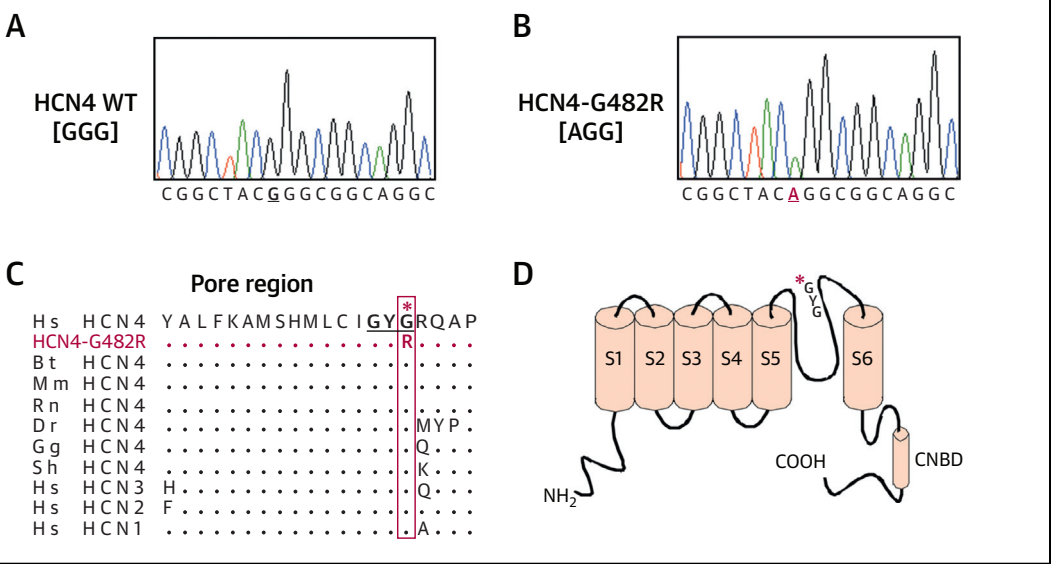

FIGURE 5 Sequence Identification of the HCN4 Mutation in the Index Family

(A, B) DNA sequence analysis of cloned wild-type (WT) and mutant DNA revealed a transition of nucleotide G1444 to A. **(C)** Conservation of residue G482 is demonstrated by amino acid sequence alignments of the HCN4 channel pore region for human, bovine, mouse, rat, zebrafish, chicken, and Tasmanian devil orthologs, and for human hyperpolarization-activated cyclic nucleotide (HCN) channels 1, 2, and 3. **(D)** Predicted HCN4 subunit topology. The mutation within the Glycine-Tyrosine-Glycine (GYG) motif of the channel pore is indicated by the **asterisk**. S = transmembrane segment.

CELLULAR PHENOTYPE OF HCN4-G482R CHANNEL SUBUNITS. Functional effects associated with the *HCN4*-G482R mutation were studied in HEK293 cells expressing HCN4 channels using the whole-cell patch clamp technique (Fig. 6A). Mutant HCN4-G482R subunits did not produce relevant hyperpolarization-activated inward currents, reflecting loss-of-function (Fig. 6A). To mimic the heteromeric configuration present in affected patients, cells were cotransfected with equal amounts of plasmid DNA encoding for wild-type and mutant HCN4 subunits. I-V relationships showed lower current densities of heteromeric compared to wild-type channels (Fig. 6B). Quantification during single voltage pulses to -120 mV (4 s) yielded wild-type HCN4-mediated current densities of -110.8 ± 15.8 pA/pF (n = 10) compared to -38.4 ± 8.8 pA/pF (n = 32) in the heteromeric configuration ($p < 0.01$) (Fig. 6C, Online Table 4). Activation and deactivation properties and reversal potential of HCN4 wild-type currents were not significantly affected by coexpression of G482R (Figs. 6D to 6F, Online Table 4). To investigate whether altered membrane trafficking could underlie current reduction, we analyzed HEK cells that expressed wild-type and mutant channels in heteromeric and homomeric configuration, using mutant constructs FLAG-tagged at the N-terminal region. Confocal microscopy showed similar surface expression of HCN4 wild-type and mutant subunits indicating equivalent trafficking (Online Fig. 4). Overlapping immunoreactivity suggested equal distribution and colocalization of wild-type and mutant FLAG-HCN4-G482R subunits.

DISCUSSION

We describe a previously unrecognized electromechanical overlap syndrome of SND and NCCM with autosomal-dominant inheritance in 2 German families and a single proband. Our approach highlights the use of NGS to uncover the underlying genetic basis of combined cardiovascular disorders. A novel *HCN4*-G482R mutation and a common *CSRP3*-W4R variant (19) were identified and found to cosegregate in the index family. Moreover, the previously reported *HCN4*-695X mutation cosegregated in the second family (11) and a *HCN4*-P883R mutation was identified in a single proband—both were clinically characterized by the combined phenotype. While HCN4 dysfunction represents an established mechanism of SND (9-12), we for the first time have linked mutations in *HCN4* to a structural cardiac defect.

MOLECULAR ELECTROPHYSIOLOGY UNDERLYING HCN4-G482R ASSOCIATED SND. The replacement of glycine by arginine (G482R) within the highly

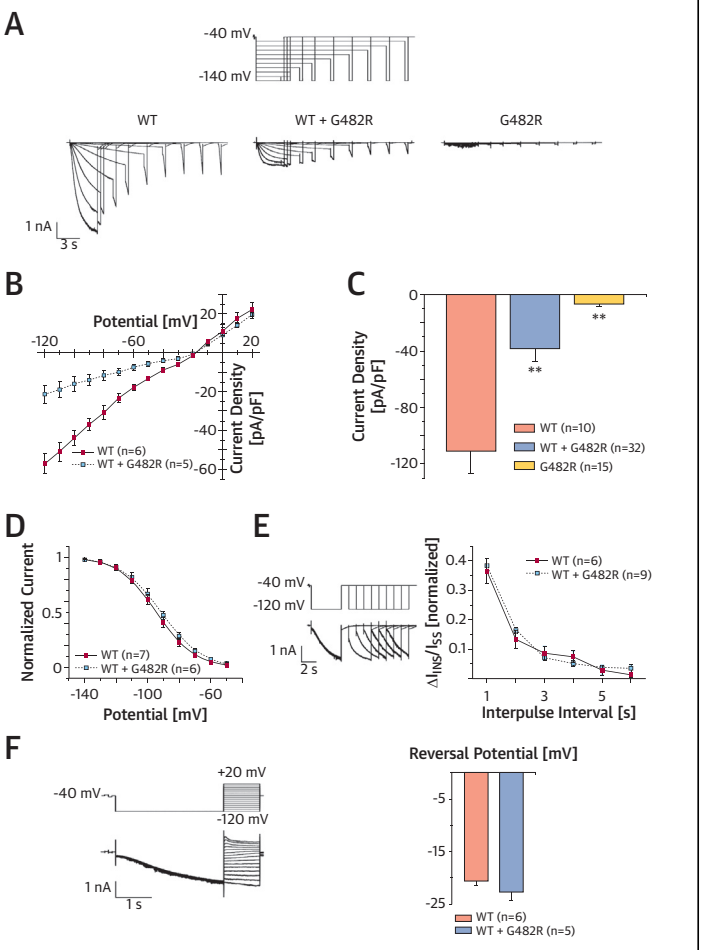

FIGURE 6 Functional Characterization of HCN4-G482R Subunits

(A) Representative current traces recorded from HEK293 cells expressing wild-type (WT), heteromeric WT-G482R, or homomeric G482R subunits using the indicated voltage protocol. **(B)** *I-V* relationships show hyperpolarization-activated cyclic nucleotide channel 4 (HCN4) current reduction in the presence of G482R subunits compared to WT channels. **(C)** Current densities determined at -120 mV membrane potential. **(D)** Activation curves of WT and heteromeric WT-G482R channels, obtained using the voltage protocol described in **A.** **(E)** Deactivation properties were examined using the indicated paired pulse protocol. Representative current traces **(left)** and resulting deactivation curves **(right)** are depicted. **(F)** Reversal potential recordings. Voltage protocol **(left, top)**, representative current traces **(left, bottom)**, and resulting mean values **(right)** are shown for indicated subunits. Data are provided as mean ± SEM. **p < 0.01.

conserved GYG motif of the channel pore (Figs. 5C and 5D) suggests a major impact on ion permeation. Accordingly, patch-clamp recordings revealed that homozygous HCN4-G482R channels were nonfunctional (Figs. 6A and 6C). Heteromeric channels composed of mutant and wild-type HCN4 subunits exhibited ~65% current reduction compared to wild-type channels (Fig. 6C), indicating a dominant-negative effect as primary mechanism of I_f current reduction in heterozygous patients. At the molecular level, current decrease may be caused by altered functional properties of the channel and/or by impaired cell surface expression. HCN4-G482R subunits did not affect surface expression of the channels (Online Fig. 4). In addition, there were no changes in activation or deactivation parameters (Figs. 6D and 6E), confirming defective ion permeation as underlying mechanism.

Carriers of *HCN4*-G482R exhibited sinus bradycardia in agreement with previous reports on HCN4 dysfunction (9,11). While slow heart rates associated with *HCN4* mutations reported were mostly asymptomatic and benign, *HCN4*-G482R carriers were severely affected and showed pronounced rate decrease leading to syncope and requiring pacemaker implantation in the index patient. The particularly severe bradycardia phenotype may be explained by dominant-negative reduction of I_f current induced by mutant HCN4-G482R subunits in the SAN.

THE MECHANISTIC SIGNIFICANCE OF HCN4 DYSFUNCTION IN NCCM. In addition to its established function in cardiac pacemaking, HCN4 was recently identified as a primary marker for cardiac progenitors of the first heart field, significantly involved in the early embryonic heart development, forming main parts of the cardiac muscle, and the conduction system (23,24). During later development, HCN4 is down-regulated in the working myocardium, and abundant expression is restricted to the SAN and the conduction system (7). Based on these findings, we hypothesize that functional HCN4 loss interferes with molecular mechanisms required during cardiac development, resulting in NCCM (Central Illustration). Myocardial compaction occurs at 5 to 8 weeks of gestation, and impairment or arrest of this process gives rise to hypertrabeculation (25). In this regard, recent data suggested that Notch-pathway disturbance causes noncompaction with congenital heart disease while sarcomere, cytoskeletal, and Z-disk mutations provoke a more myocardial disease-only phenotype (26). In support of a congenital origin both juvenile *HCN4*-G482R mutant-carriers (patients IV.1 and IV.2) exhibited marked hypertrabeculation and additional MVP early in life. Hence, a potential implication of HCN4 in signaling pathways involved in ventricular wall maturation and compaction (e.g., Notch, Neuregulin, Ephrin, or Bone morphogenic protein) (26) is of particular interest and requires future investigation.

Based on the clinical observations among our study patients, it appears surprising that no structural cardiac abnormalities were reported on HCN4 knockout mice (27). This finding may be explained

by death of homozygous animals at early embryonic stages, most likely due to failure of rate initiation (27). Heterozygous animals, however, were reported indistinguishable from wild-type littermates, while detailed post-natal structural investigations have not been performed (27). Furthermore, an absence of noncompaction phenotypes in mouse models is a previously described phenomenon (22). Luedde et al. (22) reported an NCCM-related human troponin T mutation that lacked an obvious non-compaction phenotype in their transgenic mouse model. It was speculated whether differences in species might render mice more resistant to NCCM phenotype (22). Consistent with this notion, data from other genetic cardiomyopathy models in rodents observed specific phenotypes only in certain strains (28), indicating the importance of a human-specific or at least distinctive predisposing genetic background.

POTENTIAL ROLE OF *CSRP3*-W4R IN THE INDEX FAMILY. Hetero- (patients VI.1 and VI.2) or homozygous (patient III.2) cosegregation of *CSRP3*-W4R with the clinical phenotype in the index family suggests that this variant also may contribute to the structural phenotype. However, *CSRP3*-W4R was reported prevalent in up to 1% of control probands (19,29) and has never been linked to NCCM despite its high allele frequency. Functional characterization of CSRP3-W4R using a knock-in mouse model (29) revealed that it contributes to hypertrophic cardiomyopathy and heart failure in mice. In humans, it was previously detected in dilated cardiomyopathy and hypertrophic cardiomyopathy patients but often failed to clearly segregate with either disease in families (17). Hence, it was suggested that *CSRP3*-W4R does not represent a disease-causing mutation in humans, but serves as phenotypic modifier in cardiomyopathies (18). It is reasonable to speculate in this context that the disposition to HCM associated with *CSRP*-W4R could aggravate the NCCM phenotype on the basis of an underlying *HCN4*-G482R mutation. Supporting this notion, patient III.2, who exhibited the most severe NCCM phenotype, is homozygous for *CSRP3*-W4R.

VENTRICULAR HYPERTRABECULATION IN SND PATIENTS. Whether *HCN4*-G482R alone or together with *CSRP3*-W4R underlies patients' hypertrabeculation cannot be clarified within the index family, as all affected members alive carry both mutations (Fig. 1A). To address this issue, we carried out multimodal imaging and performed mutation scans of *HCN4* in a cohort of 86 unrelated patients diagnosed for sinus bradycardia. We identified 2 additional unrelated patients that carried *HCN4* mutations and exhibited the combined phenotype: The index patient of the previously reported *HCN4*-695X mutation family (11) and a single proband that carried a heterozygous *HCN4*-P883R mutation. Of note, *CSRP3*-W4R was not present in these patients. Based on these findings, we re-evaluated the cardiac morphology of family members, carrying the *HCN4*-695X mutation and of their unaffected relatives (11) (Fig. 1B, Online Fig. 2). Although LVEF was preserved and no overt structural abnormalities were initially noted (11), all *HCN4*-695X mutant-carriers examined by comprehensive echocardiography and/or CMR exhibited biventricular hypertrabeculation (Online Fig. 2). These changes were less severe than in patients carrying *HCN4*-G482R, which might be explained by the fact that 695X compromises cAMP responsiveness of the HCN4 channel but not ion permeation itself and/or by the absence of *CSRP3*-W4R in carriers of the *HCN4*-695X mutation. Furthermore, the proband heterozygously carrying

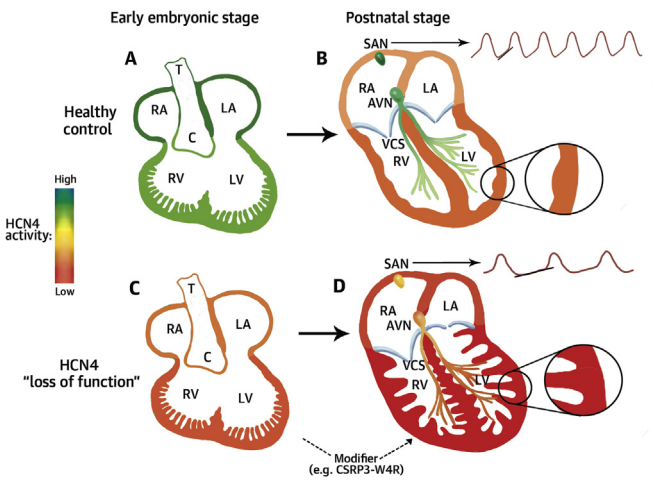

CENTRAL ILLUSTRATION Proposed Pathogenetic Process

At early embryonic stages, HCN4 is highly expressed in the immature human ventricle **(A)**, followed by down-regulation after day 30 (Carnegie stage 12) (30). At postnatal stages, significant HCN4 activity is restricted to the sinoatrial node (SAN) and the conduction system **(B)**, crucial for cardiac automaticity. We hypothesize that regular HCN4 function and expression patterning throughout early embryonic development are pre-requisites for normal ventricular wall maturation, involved in processes that regulate myocardial compaction and proper mitral valve formation **(A, B)**. HCN4 loss-of-function **(C)** may interfere with these mechanisms and hence in addition to sinus node dysfunction give rise to noncompaction and mitral valve defects **(D)**. Spatial and temporal HCN4 activity is illustrated by color. AVN = atrioventricular node; C = conus arteriosus; LA = left atrium; LV = left ventricle; RA = right atrium; RV = right ventricle; T = truncus arteriosus; VCS = ventricular conduction system.

HCN4-P883R exhibited myocardial noncompaction and was affected by SND requiring pacemaker implantation (Online Fig. 3). This case provides additional, independent evidence that validates the association of the proposed disease entity with mutations in *HCN4*. Based on these data, it appears unlikely that *CSRP3*-W4R present only in the index family serves as primary cause of the NCCM phenotype. Thus, our study strongly supports the notion that *HCN4* mutations are critically involved in the development of myocardial noncompaction.

STUDY LIMITATIONS. In this study, we did not carry out experiments on the pathogenetic role of HCN4 during heart development and the modifying contribution of the CSRP3 variant. Such studies will be necessary to elucidate the mechanistic implication of HCN4 defects in ventricular malformation and to validate its significance for NCCM.

CONCLUSIONS

We report for the first time that HCN4 channel dysfunction in addition to its known association with SND may play a distinct role in the development of structural cardiac abnormalities. The novel *HCN4* loss-of-function mutation G482R was identified and segregated with a combined disease phenotype in family members with SND and NCCM. The structural phenotype might be modified by the common *CSRP3*-W4R variant in the index family. Different *HCN4* mutations (695X and P883R) segregated with a similar combined phenotype in an unrelated family and in a single unrelated proband and further support a disease-relevant association with *HCN4*.

REPRINT REQUESTS AND CORRESPONDENCE: Dr. Patrick A. Schweizer, Department of Cardiology, University of Heidelberg, Im Neuenheimer Feld 410, 69120 Heidelberg, Germany. E-mail: patrick.schweizer@med.uni-heidelberg.de OR Dr. Dierk Thomas, Department of Cardiology, University of Heidelberg, Im Neuenheimer Feld 410, 69120 Heidelberg, Germany. E-mail: dierk.thomas@med.uni-heidelberg.de.

PERSPECTIVES

COMPETENCY IN MEDICAL KNOWLEDGE: Mutations in the *HCN4* gene are linked to a symptom complex of SND and myocardial noncompaction.

TRANSLATIONAL OUTLOOK: Future studies are required to determine the clinical utility of genetic testing and long-term cardiac rhythm monitoring in patients with myocardial noncompaction.

REFERENCES

1. Oechslin EN, Attenhofer Jost CH, Rojas JR, et al. Long-term follow-up of 34 adults with isolated left ventricular noncompaction: a distinct cardiomyopathy with poor prognosis. J Am Coll Cardiol 2000;36:493–500.

2. Oechslin E, Jenni R. Left ventricular noncompaction revisited: a distinct phenotype with genetic heterogeneity? Eur Heart J 2011;32:1446–56.

3. Luxán G, Casanova JC, Martínez-Poveda B, et al. Mutations in the NOTCH pathway regulator MIB1 cause left ventricular noncompaction cardiomyopathy. Nat Med 2013;19:193–201.

4. Hermida-Prieto M, Monserrat L, Castro-Beiras A, et al. Familial dilated cardiomyopathy and isolated left ventricular noncompaction associated with lamin A/C gene mutations. Am J Cardiol 2004;94:50–4.

5. Vatta M, Mohapatra B, Jimenez S, et al. Mutations in Cypher/ZASP in patients with dilated cardiomyopathy and left ventricular non-compaction. J Am Coll Cardiol 2003;42:2014–27.

6. DiFrancesco D, Tortora P. Direct activation of cardiac pacemaker channels by intracellular cyclic AMP. Nature 1991;351:145–7.

7. Schweizer PA, Yampolsky P, Malik R, et al. Transcription profiling of HCN-channel isotypes throughout mouse cardiac development. Basic Res Cardiol 2009;104:621–9.

8. Baruscotti M, Bucchi A, Viscomi C, et al. Deep bradycardia and heart block caused by inducible cardiac-specific knockout of the pacemaker channel gene Hcn4. Proc Natl Acad Sci U S A 2011;108:1705–10.

9. Milanesi R, Baruscotti M, Gnecchi-Ruscone T, DiFrancesco D. Familial sinus bradycardia associated with a mutation in the cardiac pacemaker channel. N Engl J Med 2006;354:151–7.

10. Schulze-Bahr E, Neu A, Friederich P, et al. Pacemaker channel dysfunction in a patient with sinus node disease. J Clin Invest 2003;111:1537–45.

11. Schweizer PA, Duhme N, Thomas D, et al. cAMP sensitivity of HCN pacemaker channels determines basal heart rate but is not critical for autonomic rate control. Circ Arrhythm Electrophysiol 2010;1:542–52.

12. Duhme N, Schweizer PA, Thomas D, et al. Altered HCN4 channel C-linker interaction is associated with familial tachycardia-bradycardia syndrome and atrial fibrillation. Eur Heart J 2013;34:2768–75.

13. Zicha S, Fernández-Velasco M, Lonardo G, et al. Sinus node dysfunction and hyperpolarization-activated (HCN) channel subunit remodeling in a canine heart failure model. Cardiovasc Res 2005;66:472–81.

14. Butters TD, Aslanidi OV, Inada S, et al. Mechanistic links between Na+ channel (SCN5A) mutations and impaired cardiac pacemaking in sick sinus syndrome. Circ Res 2010;107:126–37.

15. Holm H, Gudbjartsson DF, Sulem P, et al. A rare variant in MYH6 is associated with high risk of sick sinus syndrome. Nat Genet 2011;43:316–20.

16. Glukhov AV, Kalyanasundaram A, Lou Q, et al. Calsequestrin 2 deletion causes sinoatrial node dysfunction and atrial arrhythmias associated with altered sarcoplasmic reticulum calcium cycling and degenerative fibrosis within the mouse atrial pacemaker complex. Eur Heart J 2013 Nov 11 [E-pub ahead of print].

17. Mohapatra B, Jimenez S, Lin JH, et al. Mutations in the muscle LIM protein and alpha-actinin-2 genes in dilated cardiomyopathy and endocardial fibroelastosis. Mol Genet Metab 2003;80:207–15.

18. Newman B, Cescon D, Woo A, et al. W4R variant in CSRP3 encoding muscle LIM protein in a patient with hypertrophic cardiomyopathy. Mol Genet Metab 2005;84:374–5.

19. Bos JM, Poley RN, Ny M, et al. Genotype-phenotype relationships involving hypertrophic cardiomyopathy-associated mutations in titin, muscle LIM protein, and telethonin. Mol Genet Metab 2006;88:78–85.

20. Ludwig A, Zong X, Stieber J, et al. Two pacemaker channels from human heart with profoundly different activation kinetics. EMBO J 1999;18:2323–9.

21. Captur G, Nihoyannopoulos P. Left ventricular non-compaction: Genetic heterogeneity, diagnosis and clinical course. Int J Cardiol 2010; 140:145–53.

22. Luedde M, Ehlermann P, Weichenhan D, et al. Severe familial left ventricular non-compaction cardiomyopathy due to a novel troponin T (TNNT2) mutation. Cardiovasc Res 2010;86:452–60.

23. Liang X, Wang G, Lin L, et al. HCN4 dynamically marks the first heart field and conduction system precursors. Circ Res 2013;113:399–407.

24. Später D, Abramczuk MK, Buac K, et al. A HCN4+ cardiomyogenic progenitor derived from the first heart field and human pluripotent stem cells. Nat Cell Biol 2013;15:1098–106.

25. Towbin JA. Left ventricular noncompaction: a new form of heart failure. Heart Fail Clin 2010;6: 453–69.

26. Samsa LA, Yang B, Liu J. Embryonic cardiac chamber maturation: Trabeculation, conduction, and cardiomyocyte proliferation. Am J Med Genet C Semin Med Genet 2013;163C:157–68.

27. Stieber J, Herrmann S, Feil S, et al. The hyperpolarization-activated channel HCN4 is required for the generation of pacemaker action potentials in the embryonic heart. Proc Natl Acad Sci U S A 2003;100:15235–40.

28. Semsarian C, Healey MJ, Fatkin D, et al. A polymorphic modifier gene alters the hypertrophic response in a murine model of familial hypertrophic cardiomyopathy. J Mol Cell Cardiol 2001;33:2055–60.

29. Knöll R, Kostin S, Klede S, et al. A common MLP (muscle LIM protein) variant is associated with cardiomyopathy. Circ Res 2010;106:695–704.

30. Sizarov A, Devalla HD, Anderson RH, Passier R, Christoffels VM, Moorman AF. Molecular analysis of patterning of conduction tissues in the developing human heart. Circ Arrhythm Electrophysiol 2011;4:532–42.

KEY WORDS *HCN4*, noncompaction cardiomyopathy, overlap syndrome, sinus node dysfunction

APPENDIX For expanded Methods and References sections as well as supplemental tables, figures, and videos, please see the online version of this article.